NJC

Accepted Manuscript

This article can be cited before page numbers have been issued, to do this please use: Z. Yaseen, V. K. Aswal, X. Zhou, . Kabir-ud-Din and S. Haider, *New J. Chem.*, 2018, DOI: 10.1039/C7NJ02591B.

ROYAL SOCIETY OF CHEMISTRY

rsc.li/njc

View Article Online
DOI: 10.1039/C7NJ02591B

Journal Name

ARTICLE

Morphological changes in human serum albumin in presence of cationic amphiphilic drugs

Received 00th January 20xx,
Accepted 00th January 20xx

DOI: 10.1039/x0xx00000x

www.rsc.org/

Z. Yaseen,[a†] V. K. Aswal,[b] X. Zhou,[d] Kabir-ud-Din [c] and S. Haider [d†]

Human serum albumin (HSA) is one of the most important carrier proteins present in the blood and can constitute more than half of serum proteins. It transports various biomolecules including hormones, fatty acids, ions, drugs and functions to regulate oncotic pressure in the plasma. Cationic amphiphillic drugs like amitriptyline hydrochloride, imipramine hydrochloride and promethazine hydrochloride bind to HSA and influences function by altering its conformation, as confirmed by Small-angle neutron scattering (SANS) data coupled to dynamic light scattering measurements (DLS). Protein unfolding was observed by SANS results through an increase in the value of the radius of gyration R_g. At higher drug concentrations, there was no change in the dimensions of the protein. However, the drugs formed free aggregates at higher concentrations without any growth in the drug micelles, which was confirmed by the appearance of second peak in DLS measurements. Molecular docking revealed that the morphology of hydrophobic moiety of the cationic amphiphilic drugs decides their binding fate with HSA, while trajectories from molecular dynamics simulations highlight structural disorder in the drug-HSA complex.

Introduction

Proteins are considered to be most important, abundant and versatile macromolecules, whose functions depends on its three dimensional structure[1]. Most drugs are small compounds that target and interact with proteins to induce perturbations in the protein function[2]. The binding of a drug to bio-molecules not only provides information regarding drug action (both toxic and therapeutic) but also sheds light on disposition and transport of drugs, which are regulated by various proteins such as human serum albumin (HSA). Detailed understanding of drug-protein binding is important from structural as well as dynamic point of views. Protein binding profiles of drugs are also useful in predicting potential side effects of the drugs. Thus, an understanding of the possible interactions between drug molecules and proteins is essential, in order to develop safe-engineered and biocompatible drug delivery [3-5].

HSA is the major extracellular protein in blood plasma with a concentration of 40 mg ml^{-1}. It has high affinity for a wide range of metabolites including drugs and transports various solutes into the blood stream. Thus, functioning to maintain the pH and oncotic pressure[6]. In this context, various researchers have attempted to utilize HSA as carrier to deliver various drugs to their specific target organs, in addition to their clinical usage in hypovolemic shock treatment[7].

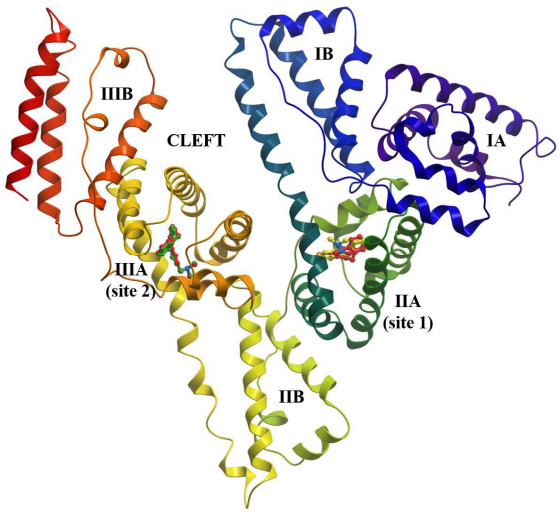

Figure 1: Structure of human serum albumin (HSA) with docked drugs. The cationic drugs bind in an orientation very similar to diclofenac (PDB id 4Z69) in site 1 and diazepam (PDB id 2BXF) in site 2. Detailed description of HSA-drug interactions in site 1/2 are illustrated in Supplementary figure S1.

[a] Department of Chemistry, Islamic University of Science and Technology, Pulwama 192 122, India
[b] Solid State Physics Division, Bhabha Atomic Research Centre, Mumbai 400 008, India
[c] Department of Chemistry, Aligarh Muslim University, Aligarh 202 002, India
[d] UCL School of Pharmacy, London WC1N 1AX, UK
† Corresponding authors
Electronic Supplementary Information (ESI) available: [details of any supplementary information available should be included here]. See DOI: 10.1039/x0xx00000x

View Article Online
DOI: 10.1039/C7NJ02591B

HSA is a single non-glycosylated, 67kD polypeptide; in globular form, the protein is composed of three structurally similar domains (I-III), each consisting of two subdomains (A and B) and stabilized by 17 disulfide bonds [7-13] (Figure 1). Several ion-pair interactions are also present at the interface region between domains (Supplementary figure S2). These ion-pair interactions and disulfide bridges impart rigidity to the structure, but at the same time, allow sufficient flexibility for the protein to undergo conformational changes based on the experimental conditions [14]. The two major binding regions of HSA, namely drug sites 1 and 2, are located in subdomains IIA and IIIA, respectively [15] (Figure 1, Supplementary figure S2). Taking into account the wide range of effective concentrations of therapeutic drugs from μM to mM and high concentration of albumin, the free concentration for a therapeutic effect can be significantly reduced for drugs with high binding to plasma. It is of interest to characterize the structure of the complexes between serum albumins and drugs in order to find out the means by which clinical efficacy of drugs can be tuned.

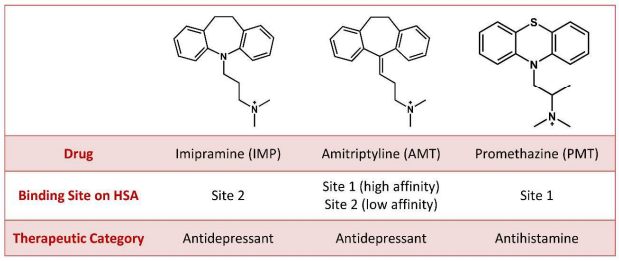

Drug	Imipramine (IMP)	Amitriptyline (AMT)	Promethazine (PMT)
Binding Site on HSA	Site 2	Site 1 (high affinity) Site 2 (low affinity)	Site 1
Therapeutic Category	Antidepressant	Antidepressant	Antihistamine

Figure 2: Chemical structures of cationic drugs imipramine hydrochloride (IMP), amitriptyline hydrochloride (AMT) and promethazine hydrochloride (PMT) used in this study.

In the present study we have used small-angle neutron scattering data (SANS) coupled with dynamic light scattering (DLS) and molecular docking and simulations (MD) to explore the structural and dynamic interactions of HSA with three cationic amphiphilic drugs (amitriptyline hydrochloride (AMT), imipramine hydrochloride (IMP) and promethazine hydrochloride (PMT); Figure 2). The group belonging to cationic amphiphilic drugs (CADs) is sizeable and includes many different therapeutic categories. Some of them are antidepressants, antiarrythmetic, antiginals, antibacterial, anoxeric, antipsychotic, and others [16]. The three drugs used here represent an interesting variety of amphiphilic structures. At one extreme they resemble with typical surfactants as they have well defined cmc (critical micelle concentration); however, they form stacked type of aggregates, unlike that of surfactants, which mostly form spheroidal aggregates [17]. The cmc values of AMT, IMP and PMT are 0.036, 0.040 and 0.045 M respectively [18]. Earlier studies on surfactant–protein binding proposed formation of micelle-like aggregates which enclose the hydrophobic patches (of the surfactant) on the protein backbone and thus result in necklace-bead structure of the protein-surfactant complex. In spite the fact that interactions between proteins and amphiphiles (especially surfactants) are well studied, the characterization of the complexes is still debated. At high surfactant concentrations, the proposed structures are: (a) "necklace and bead model" in which surfactant micelles are arranged along a polypeptide [19], (b) the rod-particle model where the amphiphile binding leads to expansion into a high aspect ratio prolate ellipsoidal [20], (c) flexible cylindrical micelle model where the protein molecule wraps around the surface of cylindrical micelles [21], and (d) a fractal arrangement of relatively small surfactant micelles bound to polypeptide chain, analogous to micellar model [22]. Characterizing the complexes between protein and amphiphilic drugs (stacked type of aggregates) is of significance from a biomedical point of view. It is also pertinent to mention that small-angle neutron scattering characterization of amphiphilic drug-protein complexes is sparsely reported in the literature.

Results and discussion

The SANS data for 1 wt % pure HSA and that of HSA incubated in the presence of the cationic drugs (from pre-micellar to post-micellar region) are shown in Figure 3. The solid lines are fit to the SANS data using an ellipsoid model with the fitted parameters listed in Table 1. The data of pure HSA has been fitted to prolate ellipsoidal model and the fitting generated a value of semi major axis (a) = 70.1Å and that of semi minor axis (b=c) = 18.2Å, which are in good agreement with that of the reported values [23]. SANS data show an increase in scattering cross-section with an increase in the drug concentration.

As observed from Figure 3A, there is continuous increase in the scattering cross-section with an increase in drug concentration and the functionality of scattering pattern of drug-protein complexes is different from that of the protein. This change in scattering pattern at low-Q values can be interpreted in terms of the unfolding of protein. Figure 3B presents the scattering data as a Kratky plot representation ($I(Q).(Q^2)$ *vs* Q) of HSA(apo) and HSA-drug complexes. Evidently, the depicted data can be grouped into two sets, low concentration regime (25 mM and 50 mM) and high concentration regime (100 mM and 200 mM). The first data set corresponds to HSA(apo) at low drug concentrations where the scattering pattern is similar to that of free HSA at high-Q values. However, there is noticeable change at low-Q values, indicating formation of larger structures. Based on the knowledge of conventional surfactant binding to the protein molecules, we tried to fit the data by using the necklace model of protein-surfactant complexes that assumes micelle-like clusters of surfactants randomly distributed along the unfolded polypeptide chain, but failed completely. The data were then fitted by using random coil Gaussian conformation, which assumes drug molecules' binding individually to the HSA, resulting in the opening of the globular protein structure into a random coil of the unfolded polypeptide chain, hence, leading to increase in the volume of the scattering particle. Data in Table 1 also suggest increase in radius of gyration (R_g) of the protein with increase in concentration of the drugs from 25 mM to 50 mM. In our earlier studies [24,25], we have reported that amphiphilic drug molecules (like AMT) form stacked type of micelles with aggregation number of 4-5 molecules, which is quite low in

View Article Online
DOI: 10.1039/C7NJ02591B

comparison to that of conventional surfactants. The low aggregation number is due to the bulky hydrophobic backbone of drug molecules. Once the drug molecules bind to the HSA molecules, the hydrophobic backbone of drug molecules gets stabilized in hydrophobic pouches of the protein (not available for the aggregation). Hence, the drug molecules individually bind to the HSA, leading to unfolding of the polypeptide chain.

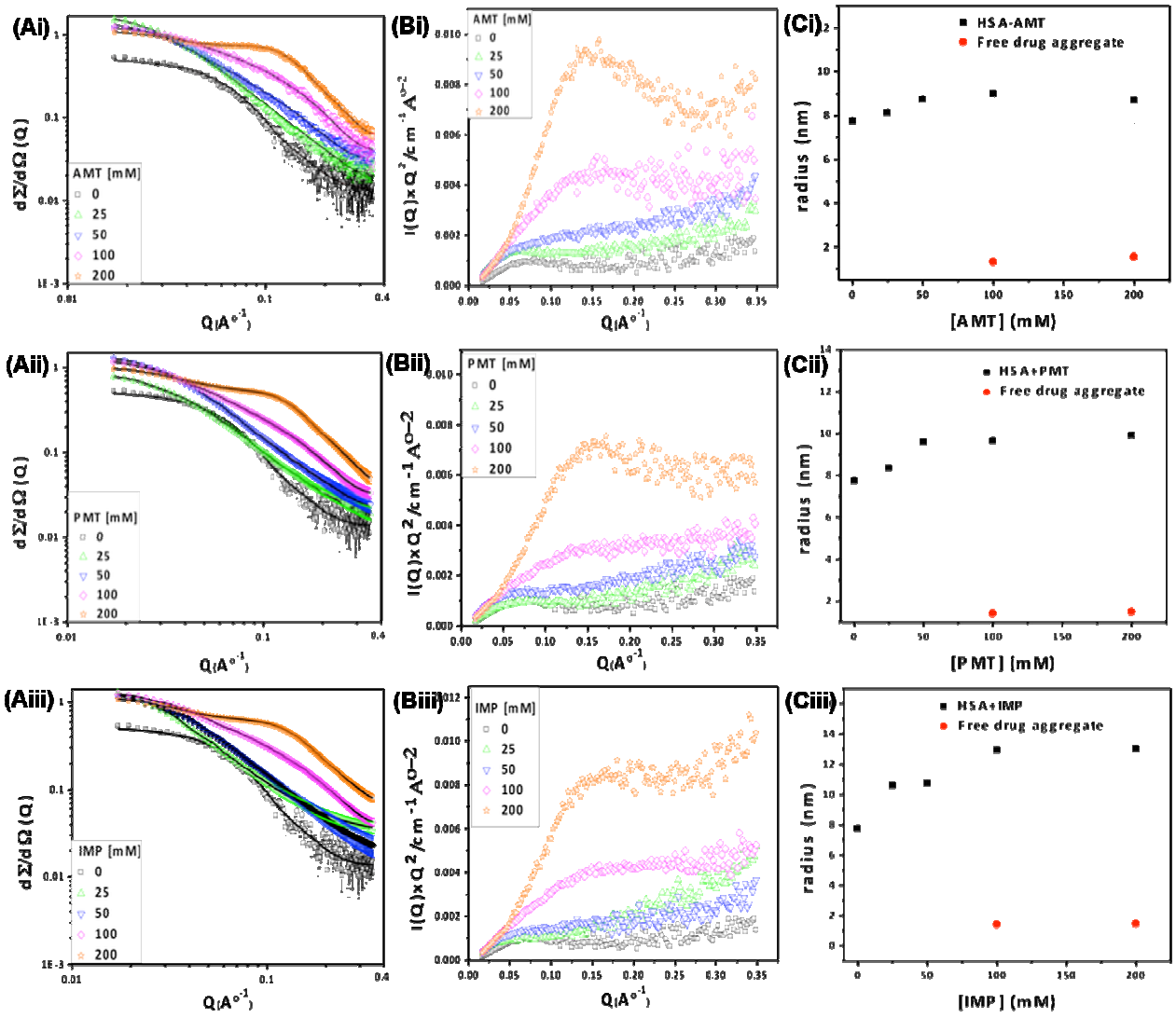

Figure 3: (A) SANS data (B) Kratky plots and (C) Average hydrodynamic radii of 1wt% HSA(apo) and HSA-drug complexes. The rows correspond to (i) HSA-AMT (ii) HSA-PMT and (iii) HSA-IMP.

Recently, Dey et al.[26] reported that at high sodium salicylate and amphihphilic sodium deoxycholate concentration, the protein fibrils rearrange to random coil conformations (sodium deoxycholate also possesses a bulky hydrophobic backbone). Kiselev et al., have reported the size of HSA in 150mM NaCl to be ~27.4 ± 0.35 Å by SANS technique[27]. The increase in Rg up to 52.88 ± 1 Å in presence of 25mM AMT (and similar changes with HSA-IMP and HSA-PMT systems, Table 1) indicates that the drug causes unfolding of the HSA molecule[28]. The drug molecules bind to the hydrophobic pockets of protein in between the sub-domains. Hence, the sub-domains of protein start separating from each other after adding the drug, which leads to increase in the values of R_g.

At higher drug concentrations (100 mM to 200 mM), the features of scattering profiles of HSA-drug complexes are very different from that of low drug concentrations. There is appearance of a correlation peak in SANS profiles of HSA-drug systems. This correlation peak is attributed to the presence of repulsive micellar aggregates, which are formed at the higher drug concentrations (the concentrations are well above the respective cmc values). Therefore, the SANS data at high drug concentrations were fitted as a sum of contributions from free micelles and HSA-drug complexes [26]. The fitted parameters are listed in Table 1. The analysis indicates that a high drug concentration does not appear to affect the HSA-

View Article Online
DOI: 10.1039/C7NJ02591B

drug complexes (as the excess drug remains in solution as free micelles without disrupting the HSA-drug complexes). Levis et al.[29] studied the influence of pH on the complex forming behaviour of amphiphilic drug nortryptyline hydrochloride and HSA, where they have reported adsorption of the drug on the protein at low drug concentrations and formation of drug aggregates at higher drug concentrations. At > 100 mM drug concentration, the correlation peak becomes more prominent indicating the presence of higher repulsive intermicellar interactions between the positively charged drug micelles. It is found that at higher drug concentrations the *Rg* value of polypeptide chain and the micellar dimensions remain the same, however, there is increase in effective particle charge (Z). An increase in scattering intensity at higher drug concentrations is due to the increase in number of free micelles.

HSA + Drug	HSA-drug complex parameters	Micellar parameters		
	R_g(Å) ± 1	*a* (Å) ± 1	*b=c* (Å) ± 1	Z
25mM AMT	52.88	-	-	-
50mM AMT	55.15	-	-	-
100mM AMT	55.03	95.59	10.93	-
200mM AMT	55.65	95.66	10.59	13.15
25mM PMT	44.59	-	-	-
50mM PMT	47.53	-	-	-
100mM PMT	57.15	97.98	10.53	-
200mM PMT	57.55	98.15	9.25	10.28
25mM IMP	42.14	-	-	-
50mM IMP	44.47	-	-	-
100mM IMP	55.12	92.23	9.82	-
200mM IMP	55.01	98.51	9.45	12.54

Table 1: Fitted parameters, i.e., semimajor axis (*a*), semiminor axis (*b,c*), radius of gyration (R_g), and effective particle charge (Z) of SANS analysis of HSA with respect to the concentration of drugs (in every system the HSA concentration was maintained constant at 1% w/v).

At low concentrations of drug (25mM and 50mM) the radius of gyration of HSA in presence of AMT increases upto a larger extent than in comparison to that of IMP and PMT (Table 1). The scattering profile in Kratky plot of HSA-AMT complex is higher than that of HSA-IMP and HSA-PMT complexes at low drug concentrations (Figure 3 B). These morphological changes of HSA in presence of AMT are attributed to the slightly large hydrophobic backbone of the AMT in comparison to that of IMP and PMT. There is literature agreement that initially the interaction between ionic compound and protein is ionic, causes the protein to unfold and exposes more binding sites [30,31]. The non-polar amino acid side chains of protein interact with hydrophobic backbone of small molecules [20.] The hydrophobic interaction of protein and small molecules leads to conformational change even when the concentration of ligand is remarkably low [32]. Higher hydrophobicity of AMT is reflected by the low critical micelle concentration of AMT in comparison to that of PMT and IMP [18]. HSA shows maximum structural change in presence of AMT upto 50mM concentration while as in case of PMT and IMP maximum changes occur up to 100mM, which is also in accordance with high hydrophobic nature of AMT.

We have also performed DLS measurements to analyze the existence of different species in solution and to obtain the size of the drug-protein complexes. Figure 3C shows the size distribution of HSA solution ([HSA] = 1% (w/v)) in the presence and absence of amphiphilic drugs. The figure collects the hydrodynamic radii of the HSA(apo) and HSA-drug complexes, taken from the position of the peaks of the intensity distribution function, at different drug concentrations. The distribution obtained for pure HSA(apo) (1wt %) solution shows one peak and hydrodynamic radius of 3.73 nm, which is in agreement with the literature value [33]. HSA-drug complexes at 25 and 50 mM drug concentrations (below cmc) also show only one peak, though the intensity and broadening of the peak indicate complex formation between the drug and HSA. The magnitude of the change in the hydrodynamic radius of HSA is sufficient to account for appreciable unfolding in the protein molecule. At 100 mM drug concentration, there is appearance of another small peak, which may be assigned to the existence of free drug aggregates. With further increase in the drug concentration (200 mM), two peaks can be perfectly distinguished, one attributable to the HSA-drug complexes and the other to the micelle-like structures formed by the drugs. This is in accordance to our SANS data, wherein also we obtained increase in size of HSA-drug complexes at small drug concentrations, and at higher concentrations, the occurrence of free drug micelles. The different values in the sizes of the complexes obtained using DLS and SANS are expected because DLS measures structures along with its hydration [23].

In an earlier study it has been reported that the unfolding in bovine serum album protein is caused by micelle-like aggregation of surfactant molecules in the complex, but in lysozyme the unfolding is due to the individual binding of the same surfactant molecules; this leads to the evidence that the model which fits to the protein-surfactant complex depends on the type of protein [34]. However, from both the studies (SANS and DLS) of HSA-drug complexes, it can be concluded that the type of model fitting to protein-amphiphile complexes depends also on the structure of the amphiphile as well.

In order to explore how AMT/PMT/IMP binds to HSA, molecular docking was performed. HSA has previously been co-crystallised with several ligands. It has been reported that AMT binds to both site 1 and 2 of HSA, while PMT only binds to site 1 and IMP shows a preference for site 2 [35-37]. Diclofenac is one of the drugs that closely resemble the cationic ligands binding in the small cavity in site 1, where AMT and PMT docked, in an orientation similar to diclofenac (Figure 1). Diazepam was used as the probe for site 2 and its common structure was used as a template to dock AMT and IMP. The calculated binding energies were similar in each site and ranged

View Article Online
DOI: 10.1039/C7NJ02591B

between HSA-AMT (-15.6 kcal/mol) and HAS-PMT (-13.2 kcal/mol) in site 1, HSA-AMT (-7.3 kcal/mol) and HSA-IMP (-6.7 kcal/mol) in site 2. The negative interaction energies suggest that the interactions are spontaneous and the morphology of hydrophobic moiety of the cationic ligands decides their binding fate. The complexes were then subjected to molecular dynamics simulations in order to extract comprehensive details concerning structural perturbations induced by the binding of cationic ligands to HSA. Three sets of statistically independent simulations for the HSA(apo) and each HSA-drug complex were run to refine the structures and investigate the morphological changes, occurring upon AMT/PMT/IMP binding. In total, 15 MD simulations were run up to 500 ns each for HSA(apo) and HSA-drug complexes. Here we report the average of the three simulations.

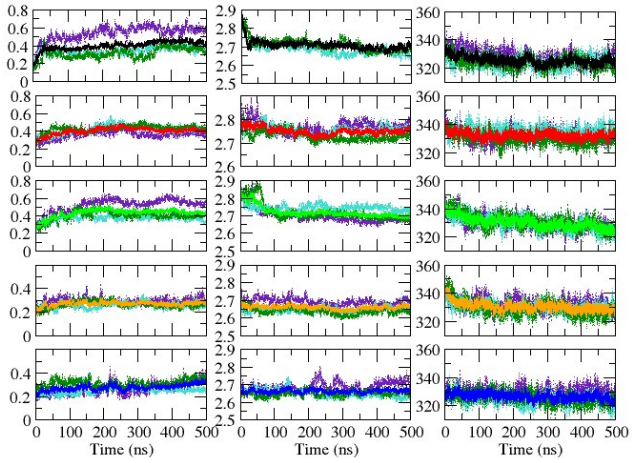

Figure 4: Left column: Cα Root mean-squared deviation (RMSD (nm)), Middle column: Radius of gyration (RG (nm)) and Right column: Solvent accessible surface area (SASA (nm^2)) of HSA(apo) (black) and in complex with AMT-site1 (red), PMT (green), AMT-site2 (orange) and IMP (blue) calculated from the simulations. Three simulations (dashed lines) for each system were run and the average values of the three simulations have been plotted (solid line).

	HSA (apo)	HSA-AMT (site 1)	HSA-PMT (site 1)	HSA-AMT (site 2)	HSA-IMP (site 2)
RMSD (nm)	0.39 (0.04)	0.43 (0.04)	0.40 (0.04)	0.27 (0.01)	0.25 (0.02)
Rg (nm)	2.69 (0.02)	2.75 (0.02)	2.72 (0.02)	2.66 (0.02)	2.65 (0.01)
SASA (nm^2)	325.5 (3.1)	332.1 (3.0)	330.2 (3.0)	330.5 (3.1)	326.7 (3.0)

Table 2: Average RMSD, Rg and SASA values over the course of the final 100ns of the simulation run. The values have been averaged over 3 simulation runs. Standard deviation is tabulated in parenthesis.

The stability of simulations was assessed by calculating the Cα root mean-squared deviation (RMSD). The radius of gyration (Rg) and solvent accessible surface (SASA) area was also monitored over the course of the simulation time to assess the tertiary structure of the systems. The values of RMSD, Rg and SASA for the final 100ns are tabulated in Table 2. The radius of gyration (Rg) measures the compactness of a protein structure. If a structure is folded, the Rg values will be stable over the course of the simulation. Native HSA maintains its tertiary structure during the simulation, although the cationic complexes stabilize at higher Rg values (Figure 4 middle column). The calculated solvent-accessible surface area (SASA) for the complexes is comparable or greater than that for native HSA indicating that the binding of cationic ligands increases the exposed areas (Figure 4 left column). AMT, when bound in site 1 displayed greatest RMSD, while the most compact structure based on Rg and SASA analysis was that of HSA(apo). A detailed view of conformational perturbation was also obtained by measuring the minimum distance of ion-pair interactions that exist at the interface between the subdomains (Supplementary figure S2B). A simultaneous, irreversible loss of multiple ion-pair interactions is an indicator of unidirectional conformational drift leading to a possible localized loss of secondary structure (Supplementary figure S3). We define these ion pair interactions collectively to be reflective of the core of the HSA structure. A total of ten ion pair interactions were monitored including R117-E520, R485-E383, R472-D494, R428-D183, R410-E492, R348-E383, R10-D259, R209-E354, K432-E184 and K432-D187. While these ion-pair interactions are reversibly maintained in the HSA(apo) simulations, the binding of cationic drugs has a noticeable destabilizing effect on most of them in the complex (Supplementary figure S2C). R485-E383 ion-pair interaction is however maintained in all systems, while R117-E520 interaction is lost only when the drugs are bound in site 2. Furthermore, a comparison of the per-residue root mean squared deviation (Supplementary figure S4) highlights the conformational drift in the drug-HSA complexes. Greater root mean squared deviation of residues is observed in the core of the complexes, as when compared with the HSA(apo). The root mean squared fluctuation also confirms that the drugs, when bound in site 1 exhibited pronounced structural effects on the protein than when bound in site 2 (Supplementary figure S5). The overall results are consistent with the experimental observation that binding of cationic ligands brings about a conformational change upon binding with HSA.

Conclusions

We have studied the effect of three cationic amphiphillic drugs (AMT/IMP/PMT) on conformation of human serum albumin (HSA). At low concentrations, the drug molecules get individually bound to HSA, and hence, the sub-domains of protein start separating from each other, resulting in increase in values of R_g (unfolding of polypeptide chain). With increase in drug concentration, there is no change in the dimensions of HSA-drug complexes. HSA in presence

View Article Online
DOI: 10.1039/C7NJ02591B

of higher drug concentrations has protein-drug complex structure with free micelles of drugs, i.e., the HSA-drug complexes coexist with free drug micelles. Both SANS and DLS studies suggest that the protein gets unfolded in presence of the cationic amphiphillic drugs, and after saturation of protein, there is formation of free micelles of the drugs (Supplementary figure S6). Molecular docking reveals that the cavities in sub-domain IIA (site 1) and IIIA (Site 2) of HSA represent the preferred binding sites to the cationic amphiphilic drugs. Thus, the hydrophobic backbone of the amphiphilic molecules (viz., the cationic drugs in the present case) plays an important role in their binding with HSA.

Experimental

Materials and methods

Amitrityline hydrochloride (AMT), promethazine hydrochloride (PMT), imipramine hydrochloride (IMP), and human serum albumin (HSA) were purchased from Sigma and used without further purification. Human serum albumin was essentially fatty acid free. All other reagents were of analytical grade. All the experiments were carried out in Tris hydrochloride buffer solution of pH=7.4.

Small-angle neutron scattering (SANS) measurements

Samples for SANS experiments were prepared by dissolving known amounts of HSA and HSA-drug mixtures in buffer solution of D_2O. The use of D_2O as a solvent (instead of H_2O) provides good contrast for the hydrogenous protein in neutron experiments. SANS is a diffraction experiment, which involves scattering of a monochromatic beam of neutrons from the sample and measuring the scattered neutron intensity as a function of the scattering angle. The wave-vector transfer Q (= $4\pi\sin\vartheta/\lambda$, where λ is the incident neutron wavelength and 2ϑ is the scattering angle) in these experiments is small, typically in the range of 10^{-3} to 1.0 Å. The wavelength of neutrons used for these experiments are usually 4–10 Å. SANS experiments were carried out at Dhruva reactor, BARC, Mumbai, India [38].

Data analysis

SANS experiments measure the coherent differential scattering cross-section (dΣ/dΩ) as a function of wave-vector transfer Q. For a system of mono-dispersed particles, it is given by [39].

$$\frac{d\Sigma}{d\Omega}(Q) = N_P V_P^2 (\rho_P - \rho_S)^2 [< F(Q)^2 > + < F(Q) >^2 [S_P(Q) - 1] + B \quad (1)$$

where V_p is the volume of the particle, ρ_P and ρs are, respectively, the scattering length densities of the particle and the solvent. N_p is the number density of the particles. $F(Q)$ is the single particle form factor and is decided by the shape and size of the particle. $S_p(Q)$ is the interparticle structure factor, which depends on the spatial arrangement of particles and on the interparticle interactions. Interparticle interference effects are negligible in case of dilute solutions (i.e. $S_p(Q)$~1). The scattered neutron intensity in the SANS experiment depends on the square of the difference between the average scattering length density of the particle and the average scattering length density of the solvent (i.e., $(\rho_P - \rho s)^2$). This term is referred to as the contrast factor. The scattering length density is positive for deuterium and negative for hydrogen, which makes SANS ideal for studying the structural aspects of hydrogenous materials such as protein solutions. B is a constant term that represents the incoherent scattering background due to hydrogen in the sample. In case of charged colloidal systems, such as protein solutions, the SANS data show a correlation peak due to interparticle structure factor indicating the presence of significant interaction between the colloids.

Modelling for HSA

In case of protein solutions of low concentrations, Eq. (1) for such systems becomes

$$\frac{d\Sigma}{d\Omega}(Q) = N_P V_P^2 (\rho_P - \rho_S)^2 < F(Q)^2 > + B \quad (2)$$

The form factor for prolate ellipsoidal shape having semi-major and minor axes a and $b=c$ can be given by

$$< F(Q)^2 > = \left[\int_0^1 F(Q,\mu) d\mu \right]^2 \quad (3)$$

$$F(Q,\mu) = \frac{3(\sin x - x\cos x)}{x^3} \quad (4)$$

$$x = Q[a^2\mu^2 + b^2(1-\mu^2)]^{1/2} \quad (5)$$

where a and b represent the semi-major and the semi-minor axes of the ellipsoidal protein macromolecules, respectively, and μ is the cosine of the angle between the directions of a and the wave-vector transfer Q.

Modelling for HSA-drug conjugates

The unfolding of protein in the presence of drugs is believed to be the opening of the globular protein structure into a random coil Gaussian conformation of the unfolded polypeptide chain. In this case, the scattering cross-section is given as

$$\frac{d\Sigma}{d\Omega}(Q) = I_o \left[Q^2 R_g^2 - 1 + \exp(-Q^2 R_g^2) \right] / \left(QR_g \right)^4 \quad (6)$$

where R_g is the radius of gyration of the unfolded protein polypeptide chain.

The interparticle structure factor $S_p(Q)$ for the charged micelles is calculated by Hayter and Penfold [40] analysis from the Ornstein-Zernike equation under the rescaled mean spherical approximation [41]. The data has been analyzed by comparing the scattering from different models to the experimental data (instrumental corrections

View Article Online
DOI: 10.1039/C7NJ02591B

were also made). The modeled scattering profiles were smeared by the appropriate resolution function to compare with the measured data. The fitted parameters in the analysis were optimized by means of nonlinear least-square fitting program [42, 43].

Dynamic light scattering (DLS)

Dynamic light scattering measurements were performed using a Laser-Spectroscatter 201 (RiNA GmbH, Berlin, Germany). In DLS measurements, a beam of laser is guided towards the sample under investigation, with a fixed detection arrangement of 90° to the center of the cell and the fluctuation in the intensity of the scattered light is measured.

Molecular docking and simulations

Structure of the HSA (PDB ID: 4Z69 and 2BXF) was downloaded from the protein data bank (http://www.rcsb.org./pdb). These structures were chosen because they are in complex with Diclofenac (4Z69, site 1) and Diazepam (2BXF, site 2), whose chemical skeleton resembles that of the studied cationic drugs. The HSA was prepared by removing diclofenac from the 4Z69 structure. The PDB files of drugs were downloaded from Drugbank (AMT DB00321; IMP D00458; PMT DB01069). The drugs were docked using the docking module in the ICM-Pro software (www.molsoft.com). Template-based docking protocol was used. The spatial orientation of the common substructure in the chemical skeletons of Diclofenac (site 1) and Diazepam (site 2) were selected as reference templates to dock the cationic drugs. Grid maps were generated around the templates, which defined a binding site encompassed in a grid of 30 x 30 x 30Å^3. Docking was run with an effort of 5, storing all alternative conformations. A maximum of 25 docked conformations were generated. The final conformation was chosen based on strongest interaction energy and the lowest rmsd values from the templates' common substructure. Visualization of the docked poses was done by using Pymol [44] and ICM-Pro Molsoft molecular modelling package. Parameters for the drugs were generated using antechamber software[45]. The complexes were set up using xleap employing ff14sb forcefield[46] for protein and GAFF for the drugs. The solvated systems were solvated using TIP3P [47] water and the edge of the box was set to at least 1 nm from the closest solute atom. The system was neutralised using K^+ and Cl^- ions. The protocol was identical for all systems. Each system was minimized and relaxed under NPT conditions for 5ns at 1 atm. The temperature was ramped upto 298K using a timestep of 4 fs, rigid bonds, a cut-off of 0.9 nm and particle mesh ewalds summation switched on for long-range electrostatics. Only the solvent and ions were allowed to move during the equilibration. The heavy atoms of the protein and ligand atoms were constrained by a spring constant set at 1 kcal/mol/Å^2. The production simulations were run using ACEMD [48] molecular dynamics engine in the NVT ensemble using a Langevin thermostat with a daming of 0.1 ps^{-1} and hydrogen mass repartitioning scheme to achieve time steps of 4fs [49]. 3 sets of simulations were run for 500 ns, for each system starting from different velocities to improve the statistics. Average rmsd of the 3 simulations was calculated and the individual simulation, closest to the average value, was chosen for further structural analysis. The rmsd values for each simulation are presented in Table S1.

Conflict of Interests

The authors have no conflict of interest.

Acknowledgements

ZY is thankful to SERB-DST, New Delhi, for Start Up Research Grant (Young Scientist) under File no. YSS/2014/000804. VKA and KUD are thankful to UGC-DAE for Research grant CSR/AO/MUM/CRS-M-147/09/464.

Notes and references

1. J.M. Berg, J.L. Tymoczko and L. Stryer, *Biochemistry*, 5th edition New York, W H Freeman, 2002.
2. S. Mizutani, E. Pauwels, V. Stoven, S. Goto and Y. Yamanishi, *Bioniformatics.* 2012, **28,** 522.
3. F. Fliri, *Nat. Chem. Biol.* 2005, **1**, 389.
4. F. Fliri, *Chem. Med. Chem*. 2007, **2**, 1774.
5. N.P. Tatonetti, *Genome Biol.* 2009, **10,** 238.
6. T.K. Maiti, K.S. Ghosh, A. Samanta, and S. Dasgupta, *J. Photochem. Photobio. A* 2008, **194**, 297.
7. S. Sugio, A. Kashima, S. Mochizuki, M. Noda, and K. Kobayashi, *Protein Eng.* 1999, **12**, 439.
8. X. M. He and D. C. Carter, *Nature.*, 1992, **358**, 209.
9. S. Curry, H. Mandelkow, P. Brick and N. Franks, *Nat. Struct. Mol. Biol.* 1998, **5**, 827.
10. S. Curry, P. Brick and N.P. Frank, *Biochim. Biophys. Acta,* 1999, **1441**, 131.
11. A.A. Bhattacharya, T. Grune and S. Curry, *J. Mol. Biol.* 2000, **303**, 721.
12. I. Petitpas, T. Grune, A. A. Bhattacharya, and S. Curry, *J. Mol. Biol.* 2001, **314**, 955.
13. J. Ghuman, P.A. Zunszain, I. Petitpas, A.A. Bhattacharya, and M. Otagiri, *J. Mol. Biol.* 2005, **353**, 38.
14. U. Anand, L. Kurup, and S. Mukherjee, *Phys. Chem. Chem. Phys.* 2012, **14,** 4250.
15. G. Sudlow, D.J. Birkett, and D.N. Wade, *Molec. Pharmac.* 1975, **11**, 824.
16. W.H. Halliwell, *Toxicol. Pathol.,* 1997, **25**, 53.
17. Z. Yaseen, M.S. Sheikh, and Kabir-ud-Din, *J. Mol. Liq.* 2013, **177**, 63.
18. S. Schreier, S.V.P. Malheiros, E. de Paula, *Biochim. Biophys. Acta,* 2000, **1508**, 210.
19. K.P Ananthapadmanabhan, In: *Interaction of surfactants with polymers and Proteins,* Eds. E.D. Goddard, P. KAnanthapadmanabhan, CRC Press, Boca Raton, FL, 1993, 319.
20. C. Tanford, *The hydrophobic effect: Formation of Micelles and Biological Membranes*, 2nd ed, Willey, New York, 1980.
21. P. Lundahi, E. Greijer, M. Sanberg, S. Cardell, and K.O. Eriksson, *Biochim. Biophys. Acta*, 1986, **873**, 20.

View Article Online
DOI: 10.1039/C7NJ02591B

22. N.J. Turro, X.G. Lei, K.P. Ananthapadmanabhan, and M. Aronson, *Langmuir.* 1995, **11**, 2525.
23. V.K. Aswal, S. Chodankar, J. Kohlbrecher, R. Vavrin, and A.G. Wagh, *Phys. Rev. E.* 2009, **80**, 011924.
24. Kabir-ud-Din and Z. Yaseen, *Colloid. Surf. B:* Biointerfaces. 2012, *93*, 208.
25. Z. Yaseen, J. Aslam, A.A. Dar and Kabir-ud-Din, Z. Phys. Chem. 2013, **227**, 459.
26. J. Dey, S. Kumar, V.K. Aswal, L.V. Panicker, K. Ismail and P.A. Hassan, *Phys. Chem. Chem. Phys.* 2015, **17**, 15442.
27. M.A. Kiselev, Iu.A. Gryzunov, G.E. Dobretsov and M.N. Komarova, *Biofizika*, 2001, **46**, 423.
28. G.H. Echols and J.W. Anderegg, *J. Am. Chem. Soc.* 1960, **82**, 5085.
29. D. Levis, S. Barbosa, D. Attwood, P. Taboado and V. Mosquera, Langmuir. 2002, **18**, 8178.
30. J.Oakes, *J. Chem. Soc. Faraday Trans. 1*, 1974, **70**, 2200
31. E. Tipping, M.N. Jones and H. A. Skinner *J. Chem. Soc. Faraday Trans. 1,* 1974, **70**,1306.
32. J. Steinhardt and J. Reynolds, *A Multiple Equilibra in proteins*, Academic press, Newyork, 1969.
33. C. Carter and X.M. He, Science. 1990, **249**, 302.
34. S.N. Chondankar, V.K. Aswal, A.G. Wagh, *AIP Conference Proceedings,* 2008, 989, 117. (doi: http://dx.doi.org/10.1063/1.2906038)
35. S.M. Sharker, A.A. Rahman, and M.A. Alam, *Insight Pharm. Sci*. 2011, **1**, 24.
36. L.L. He, Z.X. Wang, Y.X. Wang, X.P. Liu and Y.J. Yang, *Colloids Surf. B: Biointerfaces*. 2016, **145**, 820.
37. M.J. Yoo, Q.R. Smith, and D.S. Hage, *J. Chromatogr. B.* 2009, **877**, 1149.
38. V.K. Aswal, and P.S. Goyal, *Curr. Sci.* 2000, **79**, 947.
39. X.H. Guo, N.M. Zhao, S.H. Chen, and J. Teixeira, *Biopolymers.* 1990, **29**, 335.
40. J.B. Hayter, and J. Penfold, *Mol. Phys.* 1981, **4**, 109.
41. J.P. Hensen, and J.B. Hayter, *Mol. Phys.* 1982, **46**, 651.
42. J.S. Pedersen, *Adv. Colloid Interface Sci.* 1997, **70**, 171.
43. P.R. Bevington, *Data reduction and error analysis for physical sciences*, McGraw-Hill, New York, 1969.
44. W.L. DeLano, *The PyMOL Molecular Graphics System*, DeLano Scientific, San Carlos, CA, USA, 2002.
45. D.A. Case, *J. Comput. Chem.* 2005, **26**, 1668.
46. V. Hornak, R. Abel, A. Okur, B. Strockbine, A. Roitberg and C. Simmerling, *Proteins,* 2006, **65,** 712.
47. P. Mark and L. Nilsson, *J. Phys. Chem. A.* 2001, **105**, 9954.
48. M.J. Harvey, G. Giupponi and G.D. Fabritiis, *J. Chem. Theory Comput.* 2009, **5,** 1632.
49. K.A. Feenstra, B. Hess, and H.J.C. Berendsen, *J. Comput. Chem.* 1999, **20**, 786.

View Article Online
DOI: 10.1039/C7NJ02591B

Table of Contents

Sentence:

Binding of cationic amphiphillic drugs result in unfolding of Human Serum Albumin

Image: